Journal of Solid State Chemistry 181 (2008) 2924–2929

Contents lists available at ScienceDirect

Journal of Solid State Chemistry

journal homepage: www.elsevier.com/locate/jssc

Synthesis and characterisation of a novel europium-based graphite intercalation compound

Nicolas Emery [a], Claire Hérold [a,*], Christine Bellouard [b], Pierre Delcroix [a], Jean-François Marêché [a], Philippe Lagrange [a]

[a] LCSM—Nancy Université, Université Henri Poincaré Nancy I, B.P. 239, 54506 Vandoeuvre-lès-Nancy Cedex, France
[b] LPM—Nancy Université, Université Henri Poincaré Nancy I, B.P. 239, 54506 Vandoeuvre-lès-Nancy Cedex, France

ARTICLE INFO

Article history:
Received 17 April 2008
Received in revised form
29 June 2008
Accepted 13 July 2008
Available online 25 July 2008

Keywords:
Graphite
Intercalation
Europium
X-ray diffraction
^{151}Eu Mössbauer spectrometry
Magnetic interactions

ABSTRACT

In the lithium–europium–graphite system, a novel ternary compound was synthesised by direct immersion of a pyrolytic graphite platelet in a molten lithium-based alloy with a well chosen Li/Eu ratio at 400 °C. The ternary compound exhibits poly-layered intercalated sheets mainly constituted of two europium planes. Its chemical formula can be written Li_xEuC_4, since the amount of lithium is still not determined. The ^{151}Eu Mössbauer spectra clearly indicate a +II valence for europium. The magnetic susceptibility and the magnetisation versus temperature reveal a complex behaviour which is qualitatively described thanks to structural hypothesis and analogies with the magnetic properties of the binary EuC_6 compound. A first ferromagnetic transition occurring at 225 K is attributed to interactions between both intercalated europium planes. The lower temperature susceptibility behaviour can be interpreted by antiferromagnetic interactions between in-plane neighbours and ferromagnetic interactions along the *c*-axis.

1. Introduction

Lithium metal is a good intercalation vector for a few elements such as calcium, barium and europium [1]. Indeed, immersion of pyrolytic graphite platelets in lithium-based liquid alloys recently appears as an efficient method for the sample preparation of MC_6 graphite intercalation compounds (with M = Ba, Ca and Eu). Indeed, contrary to the well-known vapour phase reaction [2,3], the two steps mechanism involved in the correlated intercalation process allows the preparation of pure bulk sample. In this case, lithium intercalates first and the alloyed metal progressively eliminates and substitutes lithium leading to a binary compound. As it was already shown in the mercurographitides [4], depending on the reactions conditions, lithium and its alloyed metal can both remain in the graphite galleries leading then to a ternary compound such as $Li_3Ca_2C_6$ or $Li_{0.5}Ca_3C_6$ in the lithium–calcium–graphite system [5,6]. Taking into account the wide analogy between calcium and europium, Hérold et al. [7] have started the study of the lithium–europium–graphite system, in order to prepare novel ternary graphite intercalation compounds. Indeed, ionic radii and electronegativities of calcium and europium are very similar. Moreover, europium, as calcium, can stabilise a +II valence. These metals are able to intercalate into graphite in vapour phase but this reaction remains mainly incomplete and leads to a superficial intercalation [2,3]. On the other hand, Eu^{2+} ions holding a magnetic moment give interesting magnetic properties to the EuC_6 binary compound that were studied during the 1980s [8–10]. A review of the physical properties of GICs is given in [11]. According to the Monte-Carlo simulation of Chen et al. [10], the magnetic behaviour below the Néel temperature (T_N = 40 K) can be mainly described by in-plane antiferromagnetic and out-of-plane ferromagnetic interactions with in addition, higher-order exchange interactions.

In their preliminary studies, Hérold et al. [7] have reported the existence of two ternary graphite intercalation compounds containing lithium and europium. In the present work, a first description of the synthesis conditions, the crystal chemistry and the magnetic properties of one of them are given.

2. Synthesis

The synthesis procedure is similar to that used in the lithium–calcium–graphite system [5,6]. The first step is to weigh precisely pieces of lithium and europium in a glove box filled with a very pure argon atmosphere. Both metals are successively placed in a stainless steel reactor and heated until the formation of a well-homogenised liquid. A pyrolytic graphite platelet is then

* Corresponding author. Fax: +33 3 83 68 47 85.
E-mail address: Claire.Herold@lcsm.uhp-nancy.fr (C. Hérold).

0022-4596/$ - see front matter © 2008 Elsevier Inc. All rights reserved.
doi:10.1016/j.jssc.2008.07.024

immersed in the reactive alloy and then the reactor is tightly closed. Outside of the glove box, the reactor is arranged in a vertical furnace and heated for several days in order to reach the thermodynamical equilibrium. At the end of the reaction, the reactor is opened in a glove box, the alloy is heated to extract the sample(s) from the liquid. The sample is then cleaved and differently conditioned for each kind of characterisation. For X-ray diffraction, the sample is placed in a capillary tube sealed under argon atmosphere. For Mössbauer measurements, several pieces of sample are deposited on a mylar film, a second mylar film is then sealed on the first one in the glove box so that the sample is protected from atmosphere in an air-tight sample holder. For magnetic measurements, the sample is introduced in a silica tube sealed after introduction of a low pressure of helium.

Due to a lack of knowledge concerning the lithium–europium phase diagram, the melting point of each alloy was first approximately determined. The reaction temperature was limited to a maximum of 420 °C to avoid carbide formation. Consequently, the Li/Eu ratio of the reactive alloy needs to be higher than 1.2 to be sure that the alloy is entirely liquid. The above-mentioned ternary compound was observed in a wide range of reactive alloy compositions, since the Li/Eu ratio has to be included between 1.2 and 3. However, the best results were obtained for reactions carried out at 400 °C for 10 days with a lithium–europium alloy containing 75at% of lithium. All the following characterisations were done on samples synthesised using these conditions.

3. Crystal chemistry

The first step of the characterisation of this new graphite intercalation compound is the study of its 0 0 l X-ray diffraction pattern registered using a X-ray diffraction equipment with a reflection configuration. This diagram contains one family of 0 0 l reflections clearly indicating the presence of only one intercalated phase in the sample. From this diagram, its c-axis repeat distance was evaluated at 803 pm (Fig. 1). Very small amount of EuC_6 and metallic europium inclusions are observed in the sample. The c-axis electronic density profile was determined from the intensities of the 0 0 l reflections and compared to a c-axis stacking model which takes into account the amount of carbon and europium in the sample. Experimental and theoretical intensities and structure factors are listed in Table 1.

In this preliminary study, the amount of lithium that is not precisely known was not introduced in the model. Its very small atomic number justifies this approximation. The best agreement (residual factor: $R_F = 14\%$) was obtained for a 2 layers stacking according to the Li_xEuC_4 composition (Fig. 2). Each europium plane is distant of 244 pm from the nearest graphene sheet.

In order to determine the amount of lithium and its distribution in the graphitic framework, a nuclear microprobe experiment is required and will be done in the future. The stoichiometry of each element can be determined simultaneously [12]. Moreover, if there are some heterogeneities, they can also be put into evidence (especially that of lithium, as it was shown in [12,13]).

The $h\,k\,0$ diffraction pattern does not show any reflection. This phenomenon can be attributed either to a particular structure leading to an absence of reflection (see for example the structure of KC_8 for which the rotating crystal pattern shows only the $h\,k\,0$ reflections from graphite, [14]) or to a too large absorption of the sample. Indeed, the important atomic number of europium conducts to high X-ray absorption, not favourable to an analysis using an X-ray diffraction equipment with a transmission configuration.

Table 1
Experimental and calculated intensities and structure factors of the 0 0 l Li_xEuC_4 reflexions used in the electronic density profile calculations

Reflexion (l_c)	θ (°, Mo $K\alpha_1$)	$D_{0\,0\,l}$ (pm)	$F^{exp}_{0\,0\,l}$	$F^{calc}_{0\,0\,l}$	$I^{exp}_{0\,0\,l}$	$I^{calc}_{0\,0\,l}$
1	2.53	803	0	−9.76	0	2.93
2	5.07	401.50	−19.47	−26.80	5.77	10.93
3	7.61	267.67	100	100	100	100
4	10.17	200.75	40.70	55.68	12.18	22.80
5	12.76	160.60	−83.89	−71.37	40.38	29.23
6	15.37	133.83	52.52	57.40	12.80	15.29
7	18.01	114.71	57.72	59.53	12.80	13.61
8	20.69	100.38	−44.48	−42.41	6.40	5.81
9	23.42	89.22	0	6.81	0	0.13
10	26.21	80.30	46.40	65.79	5.12	10.29

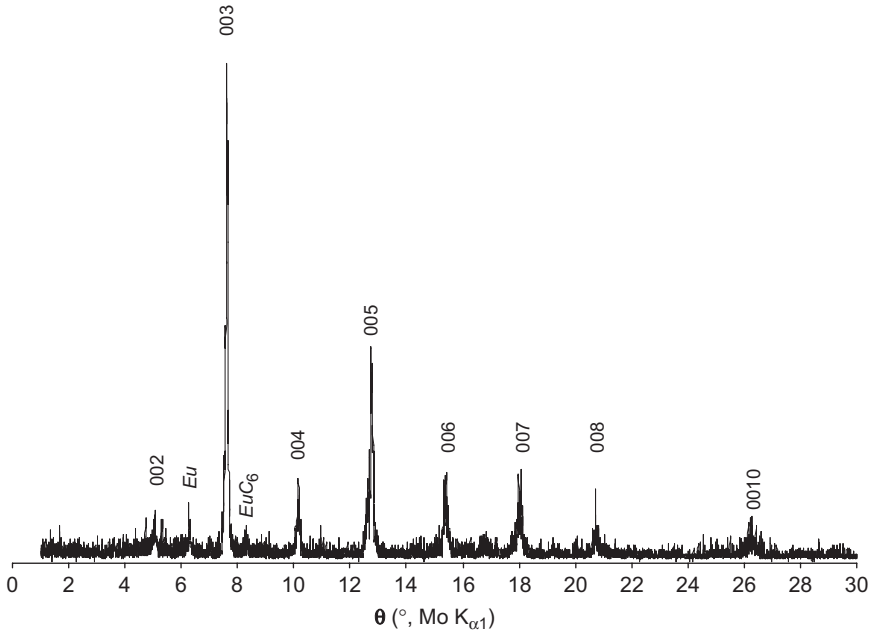

Fig. 1. 0 0 l X-ray diffraction pattern of Li_xEuC_4.

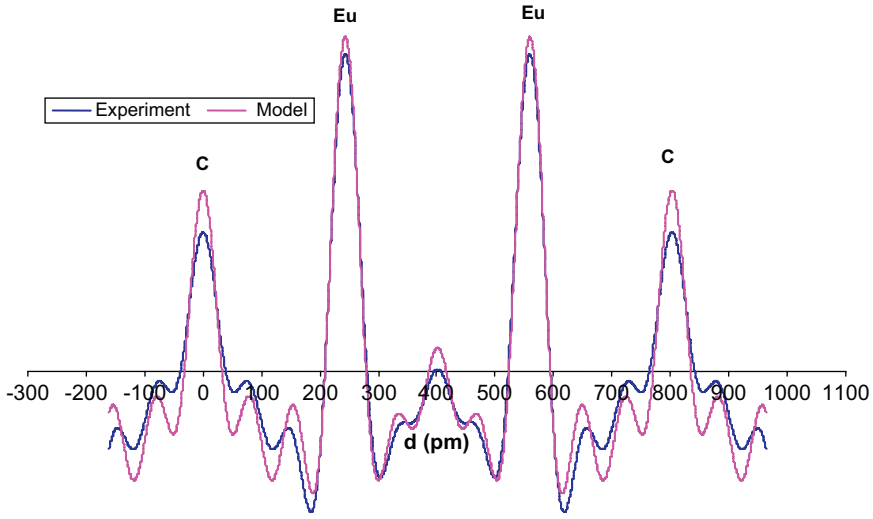

Fig. 2. 1D electronic density profiles along the *c*-axis of Li_xEuC_4.

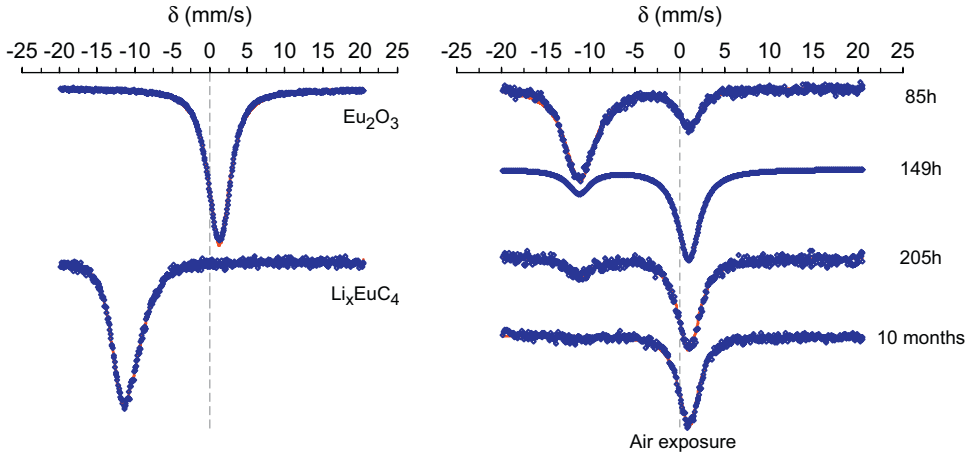

Fig. 3. ^{151}Eu Mössbauer spectra of Eu_2O_3 (Eu^{3+} used as a reference $\delta(Eu_2O_3) = 1.02$ mm/s) and of Li_xEuC_4 ($\delta(Li_xEuC_4) = -11.4$ mm/s) and the evolution of the spectra of Li_xEuC_4 under exposure to air.

4. Mössbauer spectrometry

The magnetic properties of europium-based materials are directly related to the valence of this element. In fact, the +II valence (Eu^{2+}: [Xe] $4f^7$ $6s^0$, $^8S_{7/2}$) leads to a magnetic moment $\mu = 7.94\,\mu_B$ and the +III one (Eu^{3+}: [Xe] $4f^6$ $6s^0$, $^7F_0$), to an absence of magnetic moment.

^{151}Eu Mössbauer spectrometry is a very powerful method to determine the valence of europium. Due to the highly air sensitive behaviour of this kind of materials, several platelets of Li_xEuC_4 were glued with Apiezon H® grease in a sealed mylar capsule. On one hand, the isomeric shift δ measured on the Li_xEuC_4 Mössbauer spectra reaches -11.4 mm/s (Fig. 3). This shift is related to a +II valence of europium. Moreover, the absorption peak presents an asymmetric shape that can be related to two different crystalline environments. However, more accurate measurements are needed to confirm or not this hypothesis. On the other hand, no trace of Eu^{3+} is observed on the spectra ($\delta_{Eu^{3+}} > 0$ mm/s [15]), proof of the good quality of the sample and of the air tightness of the sample holder. Indeed, the measurement has been carried out for 12 days. However, after the opening of the capsule, an absorption peak at $\delta \approx 1$ mm/s quickly appears, due to the degradation of the sample, that is to say the oxidation of europium+II in europium+III, i.e. the formation of Eu_2O_3.

5. Magnetic measurements

Magnetic susceptibility and magnetisation measurements were performed with a Physical Properties Measurement System, Quantum Design (PPMS). For the susceptibility measurements, an alternative field h of 5 Oe of frequency $f = 100$ Hz or 10 kHz was applied successively parallel and perpendicular to the *c*-axis of the graphene layers in addition to a static field H of 0 or 5000 Oe. Due to the lamellar shape of the sample, the magnetic susceptibility was corrected for the field applied parallel to the *c*-axis with the following expression where χ'_{meas} is the measured susceptibility (emu/cm^3 Oe) and D, the shape factor (in our case, D reaches 0.7 approximately):

$$\chi' = \frac{\chi'_{meas}}{1 - 4\pi D\chi'_{meas}}$$

The temperature dependence shows the same features. Susceptibility versus temperature (Fig. 4) curves show in both directions a steep increase at 225 K and a smallest one at around 44 K. A slope break is also present around 110 K. The same behaviour appears in the magnetisation measurement done with different applied fields (Fig. 5).

Susceptibility measurements of the paramagnetic phase ($T > 225$ K) have been studied in detail, in order to ensure the

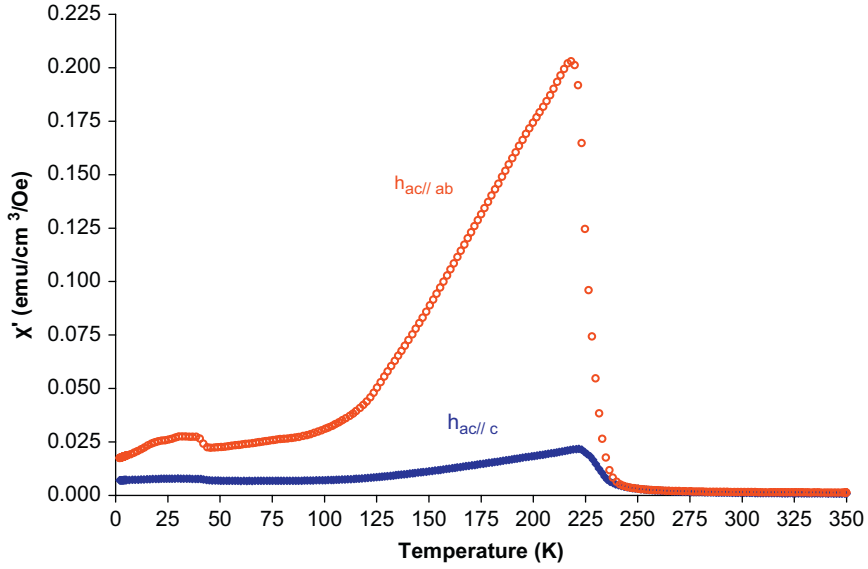

Fig. 4. Magnetic susceptibility versus temperature measured with h applied parallel and perpendicular to the c-axis ($h = 5$ Oe, $f = 100$ Hz).

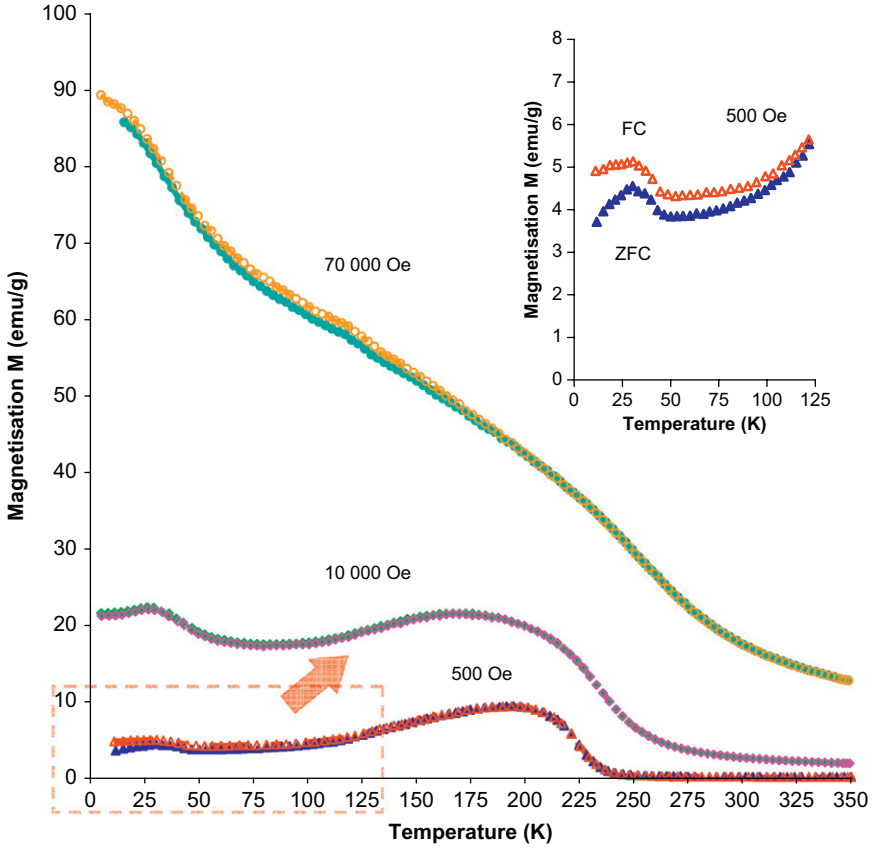

Fig. 5. Magnetisation versus temperature of Li_xEuC_4 with various applied fields ($H_{\|ab} = 500$, 10 k and 70 kOe). Open symbols are obtained from "Field Cooling" experiment (FC) and closed ones, from "Zero Field Cooling" experiment (ZFC). *Inset*: measurements done at 500 Oe below 125 K.

reliability with the structural model. The inverse of the magnetic susceptibility above 300 K has been fitted with the Curie–Weiss law and according to the definition of the Curie constant, the molar mass has been evaluated:

$$\frac{1}{\chi} = \frac{T-\theta}{C}$$
$$C = \frac{N_a \mu_{eff}^2}{3k_B M} \rightarrow M = \frac{N_a \mu_{eff}^2}{3k_B C}$$

where μ_{eff} is the effective moment of europium ($\mu_{eff} = 7.94\,\mu_B$), k_B, the Boltzmann's constant, N_a, the Avogadro's number, C and θ, the Curie's constant and the Curie's temperature, respectively, determined from the Curie–Weiss's law ($1/C_{\|c} = 27.4$ Oe g/emu K, $1/1/C_{\|ab} = 31.5$ Oe g/emu K, $\theta_{\|c} \approx 175$ K and $\theta_{\|ab} = 187$ K, Fig. 6) and M the molar mass. M evaluated from the data collected with H applied parallel to the c-axis reaches 216 g/mol. It increases until 247 g/mol using the data obtained with H applied in the perpendicular plane. According to the Li_xEuC_4 composition

proposed with the structural model, the molar mass attains $(200+xM_{Li})$ g/mol. The amount of lithium present in the structure probably does not exceed 3 atoms by formula, as it was encountered in the ternary compounds belonging to the lithium–calcium–graphite system [12,13]. This hypothesis leads to a molar mass of 221 g/mol, in good agreement with the previous values evaluated from the magnetic measurements. Of course, accurate determination of the chemical formula is still needed, as it was discussed above in the crystal chemistry section. Moreover, the proximity of the magnetic transition does not allow a more precise estimation and due to the lamellar structure of Li_xEuC_4, a small anisotropy is suggested too. This anisotropy appears clearly below the ferromagnetic transition where the initial susceptibility parallel to *c*-axis is much lower than that measured with a field parallel to the plane (Fig. 4) despite the shape factor correction.

Since the crystal structure and especially the order of the europium ions remain unknown, the magnetic behaviour cannot be quantitatively studied but, by analogy with EuC_6 and taking into account the crystallographic data, the complex magnetic behaviour of Li_xEuC_4 can be qualitatively described.

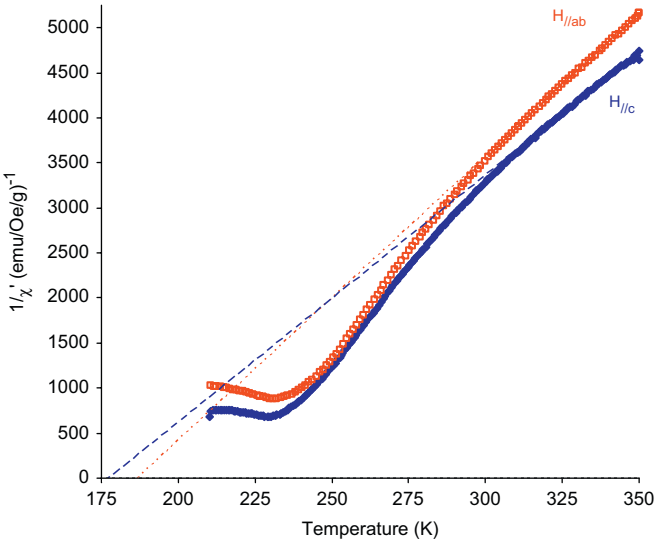

Fig. 6. Inverse of the alternative susceptibility χ' versus temperature. Data collected with $H = 5$ kOe, $h = 5$ Oe and $f = 10$ kHz.

Chen et al. [10] have shown that the main interactions in EuC_6 are antiferromagnetic between the first neighbours which are located in the same graphitic interlayer space. The interactions between two europium intercalated layers surrounding a graphene plane are ferromagnetic along the *c*-axis. The major interactions remain however antiferromagnetic, leading to a Néel temperature of 40 K (Fig. 7). According to the structural model elaborated in Section 3, in Li_xEuC_4, the distances between two europium atoms belonging to the same plane and between two europium planes surrounding a graphene sheet are very close to those in EuC_6 (Fig. 7). The main difference comes from the presence of two intercalated Eu planes (separated by 315 pm) between graphene sheets providing a lower distance between first Eu–Eu neighbours than in EuC_6 where the first neighbours are in a same plane.

The first transition observed at 225 K is attributed to a ferromagnetic transition in agreement with the positive Curie temperatures measured in the paramagnetic phase. This transition, occurring at a much higher temperature than in EuC_6, can be related to first neighbours interactions between both europium layers inside the same Van der Waals' gap.

The decrease of the magnetisation observed below 225 K until 110 K suggests the presence of antiferromagnetic interactions, related to second neighbours located in the same plane according to the structural model (Fig. 7).

The last transition observed at 44 K, leading to an increase of magnetisation can be attributed to ferromagnetic interactions between europium layers surrounding the graphene sheets. Moreover, one can see that both last interactions can be forced by a higher applied field up to 7 T (Fig. 5). Nevertheless, only half of the saturation magnetisation is reached at 5 K under 7 T.

The separation between FC and ZFC curves observed in Fig. 5 at lower temperature with a small applied field (500 Oe) can be attributed to a frustration phenomenon. Effectively, the intercalated species belonging to a same Van der Waals space probably adopts a hexagonal local ordering (triangular lattice) which leads, in the presence of antiferromagnetic interactions, to such a frustration phenomenon. This feature may also arise from competition between ferromagnetic and higher-order antiferromagnetic interactions.

Finally, the interactions diagram sketched in Fig. 7 can be directly compared to the case of EuC_6: it shows similar in-plane antiferromagnetic interactions whereas the out-of-plane

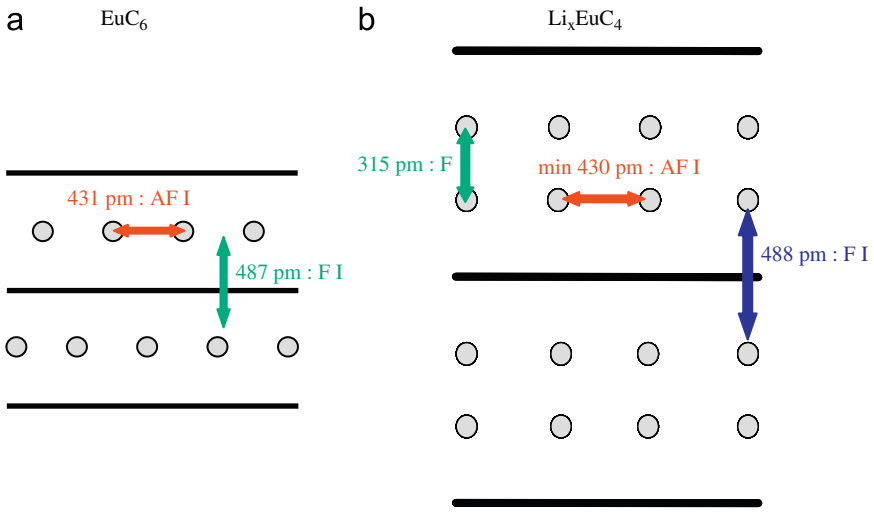

Fig. 7. *c*-Axis structural model of (a) EuC_6 and (b) Li_xEuC_4 used for the qualitative explanation of their magnetic behaviour. The distances reported are related to the distance between two successive layers along the *c*-axis or to the distance between two successive atoms of a same layer in the *ab* plane. Bold arrows represent the different magnetic interactions (AF for AntiFerromagnetic and F for Ferromagnetic).

interactions are ferromagnetic. The presence of two intercalated europium planes in each graphitic interval of Li_xEuC_4 produces prevailing ferromagnetic interactions, since the distance between these planes appears as the smallest one in this compound. On the contrary, the shortest distance between Eu atoms in the case of EuC_6 is perpendicular to the *c*-axis so that the prevailing interactions are antiferromagnetic.

6. Conclusions

As the lithium–calcium–graphite system, the lithium–europium–graphite one shows ternary phases. They are synthesised by direct immersion of pyrolytic graphite platelets in a molten lithium-based alloy. The ternary compound studied in this paper exhibits poly-layered intercalated sheets mainly constituted of two europium planes. The chemical formula of this compound can be written Li_xEuC_4, since the amount of lithium is still not determined. The Mössbauer spectra clearly indicate a +II valence for europium, leading theoretically to a magnetic moment μ_{eff} of 7.94 μ_B. The magnetic susceptibility and the magnetisation versus temperature have been investigated. Structural hypothesis and analogies with the magnetic properties of EuC_6 allow a qualitative description of the complex behaviour of Li_xEuC_4. Indeed, a first ferromagnetic transition occurring at 225 K is attributed to interactions between both intercalated Eu planes. The lower temperature susceptibility behaviour can be interpreted by antiferromagnetic interactions between in-plane neighbours and ferromagnetic interactions between planes surrounding a graphene sheet.

References

[1] N. Emery, C. Hérold, P. Lagrange, Carbon 46 (2008) 72–75.
[2] D. Guérard, M. Chaabouni, P. Lagrange, M. El Makrini, A. Hérold, Carbon 18 (1980) 257–264.
[3] M. El Makrini, D. Guérard, P. Lagrange, A. Hérold, Carbon 18 (1980) 203–209.
[4] P. Lagrange, M. El Makrini, D. Guérard, A. Hérold, Synth. Met. 2 (1980) 191–197.
[5] S. Pruvost, C. Hérold, A. Hérold, P. Lagrange, Eur. J. Inorg. Chem. (2004) 1661–1667.
[6] N. Emery, S. Pruvost, C. Hérold, P. Lagrange, J. Phys. Chem. Solids 67 (2006) 1137–1140.
[7] C. Hérold, S. Pruvost, A. Hérold, P. Lagrange, Carbon 42 (2004) 2113–2130.
[8] H. Suematsu, K. Ohmatsu, R. Yoshizaki, Solid State Commun. 38 (1981) 1103–1107.
[9] H. Suematsu, K. Ohmatsu, K. Sugiyama, T. Sakakibara, T. Motokawa, M. Date, Solid State Commun. 40 (1981) 241–243.
[10] S.T. Chen, M.S. Dresselhaus, G. Dresselhaus, H. Suematsu, H. Minemoto, K. Ohmatsu, Y. Yoshida, Phys. Rev. B 34 (1986) 423–430.
[11] T. Enoki, S. Masatsugu, E. Morinobu, Graphite Intercalation Compounds and Applications, Oxford University Press, Oxford, 2003.
[12] P. Berger, S. Pruvost, C. Hérold, P. Lagrange, NIM B 219–220 (2004) 1005–1009.
[13] S. Pruvost, P. Berger, C. Hérold, P. Lagrange, Carbon 42 (2004) 2049–2056.
[14] P. Lagrange, D. Guérard, M. El Makrini, A. Hérold, Ann. Chim. Fr. 3 (1978) 143–159.
[15] E. Kuzmann, S. Nagy, A. Vèrtes, Pure Appl. Chem. 75 (2003) 801–858.